

Optimally-Weighted Maximum Mean Discrepancy Framework for Continual Learning

KaiHui Huang^a, RunQing Wu^b, Fei Ye^{c,*}

^a*School of Software Engineering, University of Science and Technology of China*

^b*School of Mechanical Engineering, Huazhong University of Science and Technology, China*

^c*School of Information and Software Engineering, University of Electronic Science and Technology of China*

Abstract

Continual learning has emerged as a pivotal area of research, primarily due to its advantageous characteristic that allows models to persistently acquire and retain information. However, catastrophic forgetting can severely impair model performance. In this study, we tackle the issue of network forgetting by introducing a novel framework termed Optimally-Weighted Maximum Mean Discrepancy (OWMMD), which imposes penalties on representation alterations via a Multi-Level Feature Matching Mechanism (MLFMM). Furthermore, we propose an Adaptive Regularization Optimization (ARO) strategy to refine the adaptive weight vectors, which autonomously assess the significance of each feature layer throughout the optimization process. We conduct a comprehensive series of experiments, benchmarking our proposed method against several established baselines. The empirical findings indicate that our approach achieves state-of-the-art performance.

1. Introduction

Continual learning (CL) seeks to empower a model to assimilate knowledge from an ongoing influx of data, where new tasks are presented in a sequential manner [52, 55, 60, 11, 58]. A primary obstacle in CL is the phenomenon of catastrophic forgetting [35, 15, 62, 36, 57], which manifests when a model loses previously acquired knowledge while adapting to new tasks. This issue is particularly exacerbated in contexts where the model encounters limited data [46] for each task and lacks the opportunity to revisit earlier data. Various approaches have been proposed to alleviate catastrophic forgetting [56, 12], encompassing rehearsal-based techniques, regularization strategies, and architectural innovations.

Rehearsal-based approaches retain a subset of historical data and utilize it during the acquisition of new tasks [3, 61]. While these strategies facilitate the retention of knowledge from previous tasks, they frequently encounter constraints related to memory

*Corresponding author

Email address: feiye@uestc.edu.cn (Fei Ye)

capacity and computational inefficiencies. In contrast, regularization-based techniques [22] seek to mitigate substantial alterations to essential model parameters by implementing constraints that penalize significant changes. Approaches such as Elastic Weight Consolidation (EWC) [22] and Synaptic Intelligence (SI) [65] exemplify this category, demonstrating promising outcomes by safeguarding critical weights across various tasks. Nevertheless, these methodologies predominantly emphasize weight preservation and may face challenges in addressing the heterogeneous and dynamic nature of data encountered in practical applications.

Recent developments in Mixture-of-Experts (MoE) models and attention mechanisms [60] have showcased their efficacy in tackling continual learning (CL) challenges. These methodologies enable the model to allocate computational resources in a targeted manner, thereby enhancing both efficiency and performance in multi-task scenarios. However, despite these innovations, current solutions frequently encounter trade-offs related to complexity, memory consumption, and the ability to generalize across diverse tasks.

Recent advancements in continual learning have increasingly emphasized knowledge distillation-based methodologies [17, 20, 40], wherein the fundamental principle involves transferring knowledge from a previously trained model to the model currently being trained on the active task. In this context, the knowledge distillation framework typically comprises a teacher module, which is trained on the prior task and subsequently frozen, alongside a student module that undergoes continuous training on the current task. A regularization term is incorporated to minimize the divergence between the outputs of the teacher and student, thereby regulating the model’s optimization process to mitigate the risk of catastrophic forgetting. The efficacy of knowledge distillation methods is underscored by their capacity to maintain performance on earlier tasks without necessitating the retention of any memorized samples, establishing them as a prominent strategy for addressing challenges in continual learning. Nonetheless, a significant limitation of knowledge distillation approaches is their propensity to impair the learning capacity for new tasks, attributable to the issue of over-regularization.

In this paper, we tackle network forgetting in continual learning by proposing an innovative framework known as Optimally-Weighted Maximum Mean Discrepancy (OWMMD). This framework is designed to mitigate representation shifts through a probability-based distance measure. We introduce a novel Multi-Level Feature Matching Mechanism (MLFMM) that aims to minimize the distance between previously and currently learned representations throughout the model’s optimization process, effectively addressing the challenge of network forgetting. Unlike conventional distillation techniques that concentrate on aligning final outputs, MLFMM penalizes alterations in representations across all multi-level feature layers, leading to enhanced performance. To address the problem of over-regularization, MLFMM incorporates a new Adaptive Regularization Optimization (ARO) strategy that automatically assesses the significance of each feature layer during the regularization phase, thereby preventing network forgetting while facilitating the learning of future tasks. We conduct a comprehensive series of experiments and benchmark our method against several contemporary baselines. The empirical findings indicate that our proposed approach achieves state-of-the-art performance.

We summarize our main contributions in the following:

1. We present an innovative framework termed Optimally-Weighted Maximum Mean Discrepancy (OWMMD) aimed at mitigating catastrophic forgetting in continual learning paradigms. The OWMMD framework utilizes a Multi-Level Feature Matching Mechanism (MLFMM) to impose penalties on the modification of feature representations across various tasks.
2. We introduce an Adaptive Regularization Optimization (ARO) framework that enables the model to evaluate the significance of each feature layer in real-time throughout the optimization process, thereby guaranteeing optimal regularization.
3. We perform comprehensive experiments to assess the efficacy of our methodology, benchmarking it against multiple recognized baselines in continual learning. The findings indicate that our approach attains state-of-the-art performance, successfully alleviating the issue of forgetting while preserving high accuracy.

The subsequent sections of this manuscript are organized as follows: Chapter 2 provides an overview of the Related Work in continual learning, critically evaluating the advantages and drawbacks of current methodologies. Chapter 3 outlines the Methodology, elaborating on the MLFMM framework and the adaptive regularization optimization component. In Chapter 4, we detail the experimental design and outcomes, showcasing the efficacy of our approach across multiple continual learning benchmarks. Lastly, Chapter 5 wraps up the paper with a synthesis of the findings and suggestions for future research avenues.

2. Related Work

Various methods have been proposed to tackle the challenge of catastrophic forgetting, often categorizing into approaches such as rehearsal-based methods, knowledge distillation, regularization-based methods, and architecture-based methods.

Rehearsal-based methods store a small subset of past data, often referred to as an episodic memory, and replay this data during training on new tasks to retain knowledge from previous tasks [4, 9, 32]. **ER** [10] demonstrates that even very small memory buffers can significantly improve generalization. The study found that training with just one example per class from previous tasks led to improvements about 10% performance across various benchmarks, suggesting that simple memory-based methods can outperform more complex continual learning algorithms. **GEM** [32] mitigates forgetting by constraining the optimization process to avoid interference with previous tasks. GEM allows for beneficial transfer of knowledge to new tasks, showing strong performance on datasets such as MNIST [26, 37] and CIFAR-100 [45]. **A-GEM** [9] builds on GEM but improves its computational and memory efficiency, providing a better trade-off between performance and resource consumption. A-GEM also demonstrated the ability to learn more efficiently when provided with task descriptors. **GSS** [2] proposes an efficient way to select samples for replay buffers by maximizing the diversity of samples. This method frames sample selection as a constraint reduction problem, where the goal is to choose a fixed subset of constraints that best approximate the feasible region defined by the original constraints. This approach outperforms traditional task-boundary-based methods in terms of accuracy and efficiency. **HAL** [8] introduces a bilevel optimization

technique that complements experience replay by anchoring the knowledge from past tasks. By preserving predictions on anchor points through fine-tuning on episodic memory, this method improves both accuracy and the mitigation of forgetting compared to standard experience replay.

Knowledge Distillation has also been widely adopted in CL [27, 53] to combat forgetting by transferring knowledge from a "teacher" model (representing prior knowledge) to a "student" model (the current model). In Learning Without Forgetting (**LWF**) [31], a smoothed version of the teacher's output is used to guide the student's responses, ensuring that knowledge learned on previous tasks does not degrade. **iCaRL** [39] addresses class-incremental learning, where the model is required to learn from a continuously growing set of classes without access to previous data. iCaRL simultaneously learns both strong classifiers and data representations, making it suitable for deep learning architectures. The method uses knowledge distillation to retain knowledge from previous classes while adding new ones. Experiments on CIFAR-100 and ImageNet datasets show that iCaRL can effectively learn a large number of classes incrementally without forgetting previously learned ones, outperforming other methods that rely on fixed representations. Dark Experience Replay (**DER**) [4] addresses the challenges in General Continual Learning (GCL), where task boundaries are not clearly defined and the domain and class distributions may shift gradually or suddenly. The method combines rehearsal with knowledge distillation and regularization. DER works by matching the network's logits sampled throughout the optimization trajectory, thereby promoting consistency with its past outputs. In the work [48], authors investigate exemplar-free class incremental learning (CIL) using knowledge distillation (KD) as a regularization strategy to prevent forgetting. The authors introduce Teacher Adaptation (TA), a method that concurrently updates both the teacher and main models during incremental training. This method seamlessly integrates with existing KD-based CIL approaches and provides consistent improvements in performance across multiple exemplar-free CIL benchmarks.

Regularization-based methods seek to prevent catastrophic forgetting by restricting how much the model's parameters can change during training [24, 59]. **EWC** [22] presents a seminal approach for alleviating forgetting in neural networks. The method involves selective slowing down of learning on weights that are important for previous tasks. By preserving the important weights through a penalty on large weight changes, the model can continue learning new tasks while maintaining knowledge from previous ones. This regularization approach was demonstrated on both classification tasks (MNIST) and sequential learning tasks (Atari 2600 games), showing that the model can successfully retain knowledge even after long periods without encountering the original tasks. **oEWC** [43] introduces a regularization strategy within a progress and compress framework. The method works by partitioning the network into a knowledge base (which stores information about previous tasks) and an active column (which focuses on the current task). After a new task is learned, the active column is consolidated into the knowledge base, protecting the knowledge acquired so far. The key aspect of this approach is its ability to achieve this consolidation without growing the architecture, storing old data, or requiring task-specific parameters. It is shown to work effectively on sequential classification tasks and reinforcement learning domains like Atari games and maze navigation, providing a balance between learning new tasks and preserving

old knowledge. **SI** [65] mimics the adaptability of biological neural networks. In this approach, each synapse accumulates task-relevant information over time, allowing the model to store new memories while maintaining knowledge from prior tasks. The accumulated task-specific information helps the model regulate how much each synapse can change, ensuring that learning of new tasks does not interfere with older knowledge. SI significantly reduces forgetting and provides a computationally efficient method for continual learning, as demonstrated in classification tasks on benchmark datasets like MNIST. **RW** incorporates a KL-divergence-based perspective to measure the difference between the current model and the previous task’s knowledge. The method introduces two new metrics—forgetting and intransigence—to quantify how well an algorithm balances retaining old knowledge and updating for new tasks. The results show that **RW** offers superior performance compared to traditional methods, as it provides a better trade-off between forgetting and intransigence. The approach is evaluated on several benchmark datasets (MNIST, CIFAR-100), with **RW** showing significant improvement in preserving knowledge while being able to update for new tasks.

Architecture-based approaches tackle catastrophic forgetting by altering the network structure to accommodate new tasks [61, 13, 63, 18, 64, 1]. Progressive Neural Networks (**PNN**) [41] incrementally adds new modules to the network for each task, leading to a growing memory requirement. **PackNet** [33] introduces a method that allows adding multiple tasks to a single deep network by exploiting redundancies in large models through iterative pruning. This approach works by pruning a part of the network to free up parameters, which are then used for learning new tasks. The key feature of PackNet is its ability to optimize for the current task without sacrificing performance on previous tasks. Extensive experiments, such as adding multiple fine-grained classification tasks to a single ImageNet-trained VGG-16 network, demonstrate that this method provides better robustness against catastrophic forgetting compared to previous approaches that relied on proxy losses. **HAT** [44] proposes a task-based hard attention mechanism to prevent catastrophic forgetting. In this approach, a hard attention mask is learned for each task during training, allowing the network to focus on the relevant parameters for each specific task while ignoring irrelevant ones. This prevents forgetting by restricting updates to previously learned tasks. The hard attention mask is updated during training, with previous masks conditioning the learning of new tasks. This method significantly reduces forgetting and provides flexibility in controlling the stability and compactness of learned knowledge, making it suitable for both online learning and network compression applications. Quang Pham et al [38] introduce a **DualNets** framework based on the Complementary Learning Systems (CLS) theory from neuroscience, which posits that human learning occurs through two complementary systems: a fast learning system for individual experiences (hippocampus) and a slow learning system for structured knowledge (neocortex). **DualNets** implements this idea in deep neural networks by dividing the network into two components: a fast learning system for supervised learning of task-specific representations and a slow learning system for learning task-agnostic, general representations through Self-Supervised Learning (SSL). This dual approach helps the model balance learning efficiency with retention of previously learned knowledge, making it effective in both task-aware and task-free continual learning scenarios. DualNets has shown strong performance on benchmarks like CTrL, outperforming dynamic architecture methods in

Table 1: Summary of Related Works in Continual Learning.

Method Type	Description	Representative
Rehearsal-based	Store and replay past data to retain knowledge from previous tasks.	ER [10], GEM [32], A-GEM [9], GSS [2], HAL [8]
Knowledge Distillation	Transfers knowledge from a teacher model to a student model to prevent forgetting.	LWF [31], iCaRL [39], DER [34]
Regularization-based	Restricts changes to model parameters to avoid catastrophic forgetting.	EWC [22], oEWC [43], SI [65], RW [7]
Architecture-based	Alters network structure to accommodate new tasks.	PNN [41], PackNet [33], HAT [44], DualNets [38], MoE [28]

some cases. Hongbo et al explore the **MoE** [28] architecture in the context of continual learning, providing the first theoretical analysis of **MoE**'s impact in this domain. **MoE** models use a collection of specialized experts, with a router selecting the most appropriate expert for each task. The paper shows that **MoE** can diversify its experts to handle different tasks and balance the workload across experts. The study suggests that **MoE** in continual learning may require termination of updates to the gating network after sufficient training rounds for system convergence, a condition that is not required in non-continual **MoE** studies. Additionally, the paper provides insights into expected forgetting and generalization error in **MoE**, highlighting that adding more experts can delay convergence without improving performance. The theoretical insights are validated through experiments on both synthetic and real-world datasets, demonstrating the potential benefits of **MoE** in continual learning for deep neural networks (DNNs).

3. Methodology

3.1. Problem definition

In continual learning, a model is unable to access the complete training dataset simultaneously and instead acquires knowledge from a continuously evolving data stream. A common scenario in continual learning is referred to as class-incremental learning, which encompasses a sequence of N tasks $\{T_1, T_2, \dots, T_N\}$. Each task T_i is linked to a labeled training dataset $D_i^s = \{(\mathbf{x}_j^i, \mathbf{y}_j^i) \mid j = 1, \dots, N_i^s\}$, where $\mathbf{x}_j^i \in \mathcal{X}$ and $\mathbf{y}_j^i \in \mathcal{Y}$ represent the j -th paired sample from the i -th task, with N_i^s indicating the total number of samples in the training dataset D_i^s . Here, \mathcal{X} and \mathcal{Y} denote the respective spaces of data samples and labels. Additionally, let $D_i^t = \{(\mathbf{x}_j^i, \mathbf{y}_j^i) \mid j = 1, \dots, N_i^t\}$ represent the testing dataset for the i -th task, where N_i^t signifies the total number of testing samples associated with the i -th task.

In a continual learning framework, the goal of the model is to identify the optimal parameter set $\tilde{\Theta}$ that minimizes the training loss across all tasks T_1, \dots, T_i while learning the current task T_i , as expressed by the following equation :

$$\theta^* = \operatorname{argmin}_{\theta \in \tilde{\Theta}} \frac{1}{i} \sum_{k=1}^i \left\{ \frac{1}{N_i^s} \sum_{j=1}^{N_i^s} \left\{ \mathcal{L}(\mathbf{y}_j^i, f_{\theta}(\mathbf{x}_j^i)) \right\} \right\}, \quad (1)$$

where θ^* denotes the optimal model parameters, while $\mathcal{L}(\cdot, \cdot)$ represents a loss function

Table 2: Description of Mathematical Notations

Notation	Description
T_i, B_i	The i -th task in a sequence $\{T_1, T_2, \dots, T_N\}$ and number of batches of T_i .
D_i^s, D_i^t	Training/Testing datasets for task T_i : $D_i^s = \{\mathbf{x}^i, \mathbf{y}^i\}$, $D_i^t = \{\mathbf{x}^{t,i}, \mathbf{y}^{t,i}\}$.
N_i^s, N_i^t	Number of samples in D_i^s and D_i^t .
\mathcal{X}, \mathcal{Y}	Space of data samples and labels: $\mathbf{x}^i \subset \mathcal{X}$, $\mathbf{y}^i \subset \mathcal{Y}$.
$\tilde{\Theta}, \theta^*$	Set of model parameters and the optimal set found via optimization.
θ_i	The parameter of the model in T_i .
F_{θ_i}	The model with the parameter θ_i .
$F_{\theta_i, k}^{\text{feature}}$	The k -th feature layer of F_{θ_i} .
$F_{\theta_i}^{\text{classifier}}$	Linear classifier of F_{θ_i} .
\mathcal{Z}^k	Feature space of the outputs of $F_{\theta_i, k}^{\text{feature}}$.
\mathcal{Z}^c	Feature space of the last feature layer of F_{θ_i} .
$\mathcal{F}_{\text{feature}}(\theta_i, \cdot, k)$	The feature vector extracted by $F_{\theta_i, k}^{\text{feature}}$.
$f_{\theta}(\cdot)$	Classifier mapping \mathcal{X} to \mathcal{Y} .
$\mathcal{L}_s(\cdot, \cdot)$	Cross-entropy loss function.
\mathcal{M}_i	Memory buffer of T_i .
$\mathcal{F}_r(\theta_i, \theta_{i+1}, \cdot)$	A regularization term between the previous model F_{θ_i} and the current model $F_{\theta_{i+1}}$.
$F_d(\cdot, \cdot)$	Distance measure function.
α, β, γ	Coefficients that balance the importance of each term in the loss function
w_k	Adaptive weight for regularization term at the k -th layer of the network.
\tilde{w}_k	The softmax normalized weight corresponding to w_k .

that can be realized through the cross-entropy loss. Additionally, $f_{\theta}(\cdot): \mathcal{X} \rightarrow \mathcal{Y}$ functions as a classifier that receives \mathbf{x}_j^i as input and produces the corresponding predicted label.

Identifying the optimal parameter θ^* through Eq. (1) in the context of continual learning presents significant challenges, as the model is restricted to utilizing only the data samples from the current task (T_i), while all preceding tasks $\{T_1, \dots, T_{i-1}\}$ remain inaccessible. Research in continual learning seeks to devise various methodologies aimed at determining the optimal parameter that effectively minimizes the training loss across all tasks. Upon the completion of the final task (T_N), we assess the model’s performance against all testing datasets $\{D_1^t, \dots, D_N^t\}$.

3.2. Multi-Level Feature Matching Mechanism

In the realm of continual learning, numerous studies have advocated for the utilization of knowledge distillation [30, 48, 19] methodologies to mitigate the phenomenon of network forgetting. The core principle of knowledge distillation involves maintaining the previous model as a teacher module and synchronizing the outputs between the teacher and the student module, which is represented by the current classifier. This alignment seeks to minimize substantial alterations in critical parameters of the current model (student) during the acquisition of new tasks [5]. Nevertheless, the majority of existing knowledge distillation techniques primarily focus on deriving a regularization term within the prediction space, often neglecting the semantic feature space. In this paper, we present an innovative approach termed the Multi-Level Feature Matching Mechanism (MLFMM), designed to regulate information flow within the feature space, thereby aiming to avert network forgetting.

Let us formally define the function $F_{\theta_i}: \mathcal{X} \rightarrow \mathcal{Y}$ as a model parameterized by θ_i , which

comprises c feature layers denoted as $\{F_{\theta_{i,1}}^{\text{feature}}, \dots, F_{\theta_{i,c}}^{\text{feature}}\}$, along with a linear classifier represented by $F_{\theta_i}^{\text{classifier}}: \mathcal{Z}^c \rightarrow \mathcal{Y}$. Here, the index i signifies the model’s adaptation during the i -th task learning phase, and \mathcal{Z}^c refers to the feature space corresponding to the final feature layer. For a specified input \mathbf{x} , we can derive the feature vector from a particular feature layer through the following process :

$$\mathcal{F}_{\text{feature}}(\theta_i, \mathbf{x}, k) = \begin{cases} F_{\theta_{i,1}}^{\text{feature}}(\mathbf{x}) & k = 1 \\ F_{\theta_{i,k}}^{\text{feature}}(F_{\theta_{i,1}}^{\text{feature}}(\mathbf{x})) & k = 2 \\ F_{\theta_{i,k}}^{\text{feature}}(F_{\theta_{i,k-1}}^{\text{feature}}(\dots F_{\theta_{i,1}}^{\text{feature}}(\mathbf{x}))) & 3 \leq k \leq c, \end{cases} \quad (2)$$

where each feature layer $F_{\theta_{i,k}}^{\text{feature}}$ receives the output from the last layer $F_{\theta_{i,k-1}}^{\text{feature}}$ and produces the feature vector over the space \mathcal{Z}^k . The whole prediction for the model F_{θ_i} can be expressed as :

$$\hat{\mathbf{y}} = F_{\theta_i}^{\text{classifier}}(F_{\theta_{i,k}}^{\text{feature}}(F_{\theta_{i,k-1}}^{\text{feature}}(\dots F_{\theta_{i,1}}^{\text{feature}}(\mathbf{x})))), \quad (3)$$

where $\hat{\mathbf{y}}$ is the prediction for the input \mathbf{x} . In this paper, we adopt the cross-entropy loss function to update the parameter θ_i , defined by :

$$\mathcal{L}_s(\mathbf{y}, \hat{\mathbf{y}}) = \sum_{t=1}^{\mathbb{C}} \{ \mathbf{y}[t] \log(\hat{\mathbf{y}}[t]) \}, \quad (4)$$

where \mathbb{C} is the total number of classes.

To mitigate the issue of network forgetting, this study implements a memory buffer \mathcal{M}_i to retain a limited number of historical examples. In particular, we propose utilizing reservoir sampling for the sample selection process, which offers computational efficiency. Nonetheless, the model’s performance on prior tasks diminishes when the memory capacity is constrained. To tackle this challenge, the proposed MLFMM regulates the updates to the model’s representations during the learning of new tasks. Specifically, upon the completion of the current task T_i , we preserve and freeze the parameters of all feature layers $\{F_{\theta_{i,1}}^{\text{feature}}, \dots, F_{\theta_{i,c}}^{\text{feature}}\}$ during the subsequent task learning T_{i+1} . A regularization term is incorporated to minimize the discrepancy in representations between the previous model F_{θ_i} and the current model $F_{\theta_{i+1}}$ at T_{i+1} :

$$\mathcal{F}_r(\theta_i, \theta_{i+1}, \mathbf{x}) = \sum_{t=1}^c \left\{ F_d(\mathcal{F}_{\text{feature}}(\theta_i, \mathbf{x}, t), F_d(\mathcal{F}_{\text{feature}}(\theta_{i+1}, \mathbf{x}, t))) \right\}, \quad (5)$$

where $F_d(\cdot, \cdot)$ is a distance measure function and c is the total number of feature layers. In the following section, we introduce a probabilistic distance to implement Eq. (5).

3.3. The Maximum Mean Discrepancy based Regularization

Maximum Mean Discrepancy (MMD) serves as a significant and widely utilized distance metric within the realm of machine learning, grounded in a kernel-based statistical framework designed to assess the equivalence of two data distributions. Owing to its robust distance estimation capabilities, MMD has been adopted as a fundamental loss function for training diverse models across various applications, including image synthesis and density estimation. In contrast to alternative distance metrics such as

Kullback–Leibler (KL) divergence and Earth Mover’s Distance, the principal advantage of the MMD criterion lies in its incorporation of the kernel trick, which facilitates the estimation of MMD on vectors without necessitating knowledge of the specific form of the density function.

The Maximum Mean Discrepancy (MMD) criterion is predicated on the concept of embedding probability distributions within a Reproducing Kernel Hilbert Space (RKHS). Let us denote A and B as two Borel probability measures. We introduce \mathbf{a} and \mathbf{b} as random variables defined over a topological space \mathcal{X} . Furthermore, we characterize the set $\{f \in \mathcal{F} | f: \mathcal{X} \rightarrow \mathbf{R}\}$ as a function, where \mathcal{F} represents a specific class of functions. The MMD criterion quantifying the divergence between the distributions A and B is articulated as [49] :

$$\mathcal{L}_M(A, B) \triangleq \sup_{f \in \mathcal{F}} (\mathbb{E}_{\mathbf{a} \sim A} [f(\mathbf{a})] - \mathbb{E}_{\mathbf{b} \sim B} [f(\mathbf{b})]) . \quad (6)$$

where $\sup(\cdot)$ indicates the least upper bound of a set of numbers. If two distribution are same $A = B$, we can have $\mathcal{L}_M(A, B) = 0$. The function class \mathcal{F} is implemented as a unit ball in an RKHS with a positive definite kernel $f_k(\mathbf{a}, \mathbf{a}')$. Eq. (6) is usually hard to be calculated, it can be estimated on the embedding space [14], which is defined as :

$$\mathcal{L}_M^2(A, B) = \|\boldsymbol{\mu}_A - \boldsymbol{\mu}_B\|^2 , \quad (7)$$

where $\boldsymbol{\mu}_A$ and $\boldsymbol{\mu}_B$ are the mean embedding of the two distributions A and B , respectively. $\|\cdot\|^2$ is the Euclidean distance. Each mean embedding $\boldsymbol{\mu}_A$ is defined as :

$$\boldsymbol{\mu}_A = \int f_k(\mathbf{a}, \cdot) \frac{\partial P(\mathbf{a})}{\partial \mathbf{a}} d\mathbf{a} , \quad (8)$$

where $P(\mathbf{a})$ is the probability density function for the distributioin A . Each mean embedding $\boldsymbol{\mu}_P$ also satisfies the following equation :

$$\mathbb{E}[f(\mathbf{a})] = \langle f, \boldsymbol{\mu}_A \rangle_{\mathcal{H}} , \quad (9)$$

where $\langle f, \cdot \rangle_{\mathcal{H}}$ is the inner product. Specifically due to the reproducing property of RKHS $f \in \mathcal{F}, f(\mathbf{a}) = \langle f, f_k(\mathbf{a}, \cdot) \rangle_{\mathcal{H}}$, we can solve Eq. (7) by considering the kernel functions:

$$\mathcal{L}_M^2(A, B) = \mathbb{E}_{\mathbf{a}, \mathbf{a}' \sim A} [f_k(\mathbf{a}, \mathbf{a}')] - 2\mathbb{E}_{\mathbf{a} \sim P, \mathbf{b} \sim B} [f_k(\mathbf{a}, \mathbf{b})] + \mathbb{E}_{\mathbf{b}, \mathbf{b}' \sim B} [f_k(\mathbf{b}, \mathbf{b}')] , \quad (10)$$

where \mathbf{a}' and \mathbf{b}' denotes independent copies of the samples \mathbf{a} and \mathbf{b} , respectively. In practice, we usually collect the same number of samples from the two distributions A and B ($N_A = N_B = N$), where N_A and N_B denote the number of samples from two distributions A and B , respectively. We can estimate Eq. (10) by considering an unbiased empirical measure:

$$\mathcal{L}_M^e(A, B) = \frac{1}{N(N-1)} \sum_{i=1}^N \sum_{i \neq j} \left\{ h(i, j) \right\} , \quad (11)$$

where $h(i, j) = f_k(\mathbf{a}_i, \mathbf{a}_j) + f_k(\mathbf{b}_i, \mathbf{b}_j) - f_k(\mathbf{a}_i, \mathbf{b}_j) - f_k(\mathbf{a}_j, \mathbf{b}_i)$. To apply Eq. (11) for the

proposed regularization term defined in Eq. (5), we first form a set of feature vectors, expressed as :

$$\mathbf{Z}_i = \{\mathbf{Z}_i^1, \dots, \mathbf{Z}_i^c\}, \quad (12)$$

where each \mathbf{Z}_i^j is a feature vector formed using a batch of data samples $\{\mathbf{x}_1, \dots, \mathbf{x}_b\}$, expressed as :

$$\mathbf{Z}_i^j = \{\mathcal{F}_{\text{feature}}(\theta_i, \mathbf{x}_1, j), \dots, \mathcal{F}_{\text{feature}}(\theta_i, \mathbf{x}_b, j)\}, \quad (13)$$

Similar, we can form the feature vector \mathbf{Z}_{i+1}^j using the current model F_{θ_i} on the data batch $\{\mathbf{x}_1, \dots, \mathbf{x}_b\}$, expressed as :

$$\mathbf{Z}_{i+1}^j = \{\mathcal{F}_{\text{feature}}(\theta_{i+1}, \mathbf{x}_1, j), \dots, \mathcal{F}_{\text{feature}}(\theta_{i+1}, \mathbf{x}_b, j)\}. \quad (14)$$

Let $P_{\mathbf{Z}_i^j}$ and $P_{\mathbf{Z}_{i+1}^j}$ denote the distribution of \mathbf{Z}_i^j and \mathbf{Z}_{i+1}^j , respectively. Based on the MMD criterion and Eq. (5), we can implement the regularization function when seeing the data batch $\{\mathbf{x}_1, \dots, \mathbf{x}_b\}$ at the new task learning \mathcal{T}_{i+1} as :

$$\mathcal{L}_r = \sum_{t=1}^c \left\{ \mathcal{L}_M^e(P_{\mathbf{Z}_i^t}, P_{\mathbf{Z}_{i+1}^t}) \right\}. \quad (15)$$

Furthermore, we propose utilizing the **DER++** [4] as our foundational model while incorporating the suggested regularization term into the primary objective function. The **DER++** framework integrates rehearsal, knowledge distillation, and regularization techniques to effectively tackle General Continual Learning (GCL) challenges [16, 29]. This approach ensures that the predictions of the current model are aligned with those from previous tasks through a composite of loss components: the conventional loss associated with the current task, a regularization term, and a distillation term :

$$\begin{aligned} \mathbb{E}_{(\mathbf{x}, \mathbf{y}) \sim P_{D_{i+1}^s}} [\mathcal{L}_s(\mathbf{y}, F_{\theta_{i+1}}(\mathbf{x}))] + \alpha \mathbb{E}_{(\mathbf{x}, \mathbf{z}) \sim P_{\mathcal{M}_{i+1}}} [||\mathbf{z} - H_{\theta_{i+1}}(\mathbf{x})||^2] \\ + \beta \mathbb{E}_{(\mathbf{x}, \mathbf{y}) \sim P_{\mathcal{M}_{i+1}}} [\mathcal{L}_s(\mathbf{y}, F_{\theta_{i+1}}(\mathbf{x}))] \end{aligned} \quad (16)$$

where $P_{D_{i+1}^s}$ and $P_{\mathcal{M}_{i+1}}$ denote the distribution of D_{i+1}^s and the memory buffer \mathcal{M}_{i+1} at the $(i+1)$ -th task learning, \mathbf{z} is the corresponding pre-softmax responses (logits). Thus, we have $F_{\theta}(x) \triangleq \text{softmax}(H_{\theta}(x))$. This approach helps the model retain past knowledge while learning new tasks efficiently.

Since the proposed approach can be smoothly applied to the existing continual learning models, we consider applying our approach to **DER++**. The final objective function, including a regularization term \mathcal{L}_r , is defined as :

$$\begin{aligned} \mathcal{L}_{\text{total}} = \mathbb{E}_{(\mathbf{x}, \mathbf{y}) \sim P_{D_{i+1}^s}} [\mathcal{L}_s(\mathbf{y}, F_{\theta_{i+1}}(\mathbf{x}))] + \alpha \mathbb{E}_{(\mathbf{x}, \mathbf{z}) \sim P_{\mathcal{M}_{i+1}}} [||\mathbf{z} - H_{\theta_{i+1}}(\mathbf{x})||^2] \\ + \beta \mathbb{E}_{(\mathbf{x}, \mathbf{y}) \sim P_{\mathcal{M}_{i+1}}} [\mathcal{L}_s(\mathbf{y}, F_{\theta_{i+1}}(\mathbf{x}))] + \gamma \mathcal{L}_r, \end{aligned} \quad (17)$$

where γ is a hyperparameter to control the importance of the regularization term.

3.4. Adaptive Regularization Optimization Term

To improve the efficacy of the proposed MMD-based regularization method [47, 49], it is essential to automatically allocate distinct weights to each regularization term. This

strategy enables the assignment of varying degrees of significance to the features derived from different layers, thereby accurately reflecting their contributions to the overall learning framework. Specifically, we can establish an adaptive weight for each layer to assess its relevance to the entire learning process. To ensure that the adaptive weights across all layers are normalized and suitably balanced, we incorporate the softmax function.

Let $\mathbf{w} = \{w_1, \dots, w_c\}$ be a trainable adaptive weight vector, where w_j determines the importance of the j -th feature layer. To avoid numerical overflow, we propose to normalize all weights using the following equation :

$$\tilde{w}_j = \frac{e^{w_j}}{\sum_{k=1}^c \{e^{w_k}\}}, \quad (18)$$

where \tilde{w}_j is the normalized value of the j -th adaptive weight w_j . By using the normalized adaptive weights, the regularization function can be redefined as :

$$\mathcal{L}'_r = \sum_{t=1}^c \left\{ \tilde{w}_j \mathcal{L}'_M(P_{\mathbf{z}^t}, P_{\mathbf{z}^{t+1}}) \right\}. \quad (19)$$

The final loss function is redefined as :

$$\begin{aligned} \mathcal{L}'_{\text{total}} = & \mathbb{E}_{(\mathbf{x}, \mathbf{y}) \sim P_{D_{i+1}^s}} [\mathcal{L}_s(\mathbf{y}, F_{\theta_{i+1}}(\mathbf{x}))] + \alpha \mathbb{E}_{(\mathbf{x}, \mathbf{z}) \sim P_{\mathcal{M}_{i+1}}} [||\mathbf{z} - F_{\theta_{i+1}}(\mathbf{x})||^2] \\ & + \beta \mathbb{E}_{(\mathbf{x}, \mathbf{y}) \sim P_{\mathcal{M}_{i+1}}} [\mathcal{L}_s(\mathbf{y}, F_{\theta_{i+1}}(\mathbf{x}))] + \gamma \mathcal{L}'_r, \end{aligned} \quad (20)$$

During the training procedure, each adaptive weight w_j is optimized by :

$$w_j = w_j - \eta \nabla \mathcal{L}'_{\text{total}}, j = 1, \dots, c. \quad (21)$$

where η is the learning rate.

3.5. Algorithm Implementation

The proposed framework is implemented in two main stages. First, we train the model on a sequence of tasks by minimizing a total loss function that consists of several components. The training procedure starts with the input dataset D , model parameters θ , scalars α , β , and γ , learning rate η , and the number of model layers c . Initially, the memory buffer \mathcal{M} is empty, and the adaptive weight vector \mathbf{w} is initialized with values sampled uniformly from a range of 0 to 1 for each feature layer. The training proceeds iteratively through each task, updating the total loss function at every step. During training, the model’s weights and the adaptive weights are optimized using gradients computed from the total loss function.

In each iteration of the algorithm, for each data point in the dataset, the model computes a total loss that includes three terms. The first term is the standard loss function \mathcal{L}_s , which evaluates the model’s prediction against the ground truth. The second term is a distance-based regularization, defined by the squared Euclidean distance between the current task’s feature representation and an exemplar from the memory buffer. The third term, which is computed only after the first task, incorporates the adaptive regularization term \mathcal{L}'_r . This term quantifies the discrepancy between the feature layer

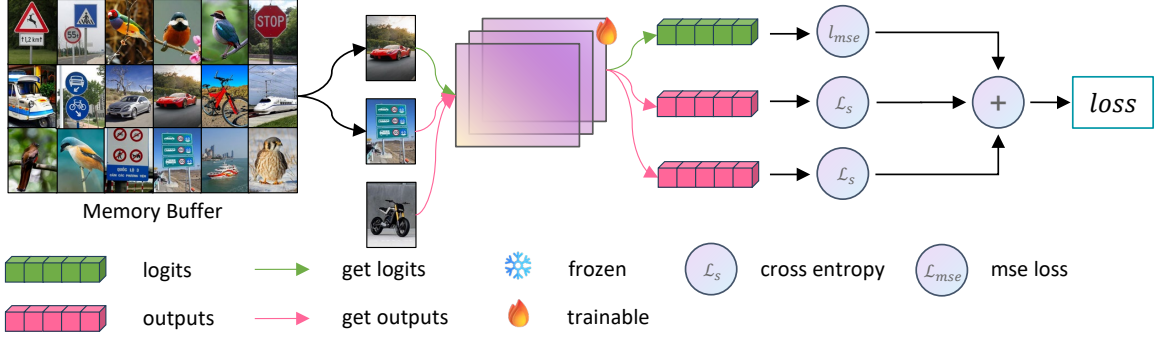
Algorithm 1 The training algorithm of the proposed MLFMM framework

```
1: Input : dataset  $D$ , parameters  $\theta$ , scalars  $\alpha$ ,  $\beta$  and  $\gamma$ , learning rate  $\eta$ , number of
   model layers  $c$ 
2: Init :  $\mathcal{M} \leftarrow \{\}$ ,  $\mathbf{w} \leftarrow \mathbf{Uniform}(\mathbf{0}, \mathbf{1}, \mathbf{c})$ 
3: for  $i = 1$  to  $N$  do
4:   for  $(\mathbf{x}, \mathbf{y})$  in  $D_i^s$  do
5:      $\mathcal{L}_{\text{total}} \leftarrow \mathcal{L}_s(y, F_\theta(\mathbf{x}))$ 
6:      $\mathbf{z} \leftarrow H_\theta(\mathbf{x})$ 
7:      $(\mathbf{x}', \mathbf{z}') \leftarrow \mathbf{sample}(\mathcal{M})$ 
8:      $\mathcal{L}_{\text{total}} \leftarrow \mathcal{L}_{\text{total}} + \alpha \cdot \|\mathbf{z}' - H_\theta(\mathbf{x}')\|^2$ 
9:      $(\mathbf{x}', \mathbf{y}') \leftarrow \mathbf{sample}(\mathcal{M})$ 
10:     $\mathcal{L}_{\text{total}} \leftarrow \mathcal{L}_{\text{total}} + \beta \cdot \mathcal{L}_s(y', F_\theta(\mathbf{x}'))$ 
11:    if  $i > 1$  then
12:       $\mathbf{x}' \leftarrow \mathbf{sample}(\mathcal{M})$ 
13:       $\mathcal{L}_{\text{total}} \leftarrow \mathcal{L}_{\text{total}} + \gamma \cdot \mathcal{L}'_r(\mathbf{x}')$ 
14:       $\theta \leftarrow \theta - \eta \nabla \mathcal{L}_{\text{total}}$ 
15:       $\mathbf{w} \leftarrow \mathbf{w} - \eta \nabla \mathcal{L}_{\text{total}}$ 
16:    else
17:       $\theta \leftarrow \theta - \eta \nabla \mathcal{L}_{\text{total}}$ 
18:    end if
19:     $\mathcal{M} \leftarrow \mathbf{reservoir}(\mathcal{M}, (\mathbf{x}, \mathbf{y}, \mathbf{z}))$ 
20:  end for
21: end for
```

outputs of the Teacher network (trained on the last task T_{i-1}) and the Student network (currently training on the current task T_i) by calculating the distance between the features \mathcal{F}_\square and \mathcal{F}_f from corresponding layers of both networks. These distances are weighted by the normalized adaptive weights \tilde{w}_k , ensuring that each layer’s contribution to the regularization term is appropriately scaled.

The optimization of model parameters θ and adaptive weights \mathbf{w} is performed using gradient descent, where the gradients of the total loss function are computed with respect to both the model parameters and the adaptive weights. The memory buffer \mathcal{M} is updated using a reservoir sampling strategy [51], which stores the most relevant samples from the current task’s data. This procedure ensures that the memory buffer contains a balanced mix of data from both current and past tasks. The algorithm continues iteratively until all tasks have been processed, with the final model achieving continual learning across the entire sequence of tasks.

As shown in Figure 1, the process for the first task involves the model learning from the initial task without applying the adaptive regularization term. During this phase, the model focuses solely on the current task’s loss function without considering past tasks. In subsequent tasks ($i > 1$), as depicted in Figure 2, the model begins to incorporate the adaptive regularization term \mathcal{L}_r , which helps prevent forgetting while learning new tasks. This process ensures that the model retains knowledge from previous tasks by leveraging adaptive weights that regulate the influence of each layer in the network. Figure 3 illustrates how the \mathcal{L}_r term is computed, showing the weighted distances



Algorithm 2 Adaptive Regularization Optimization Term for T_i

- 1: **Input** : input data \mathbf{x} , adaptive weights \mathbf{w}
 - 2: $w_{sum} \leftarrow 0$
 - 3: **for** $j = 1$ **to** c **do**
 - 4: $w_{sum} \leftarrow w_{sum} + e^{w_j}$
 - 5: **end for**
 - 6: $d \leftarrow 0$
 - 7: $\mathcal{F}_t \leftarrow \mathbf{x}$
 - 8: $\mathcal{F}_s \leftarrow \mathbf{x}$
 - 9: **for** $k = 1$ **to** c **do**
 - 10: $\mathcal{F}_t, \mathcal{F}_s \leftarrow F_{\theta_{i-1,k}}^{\text{feature}}(\mathcal{F}_t), F_{\theta_{i,k}}^{\text{feature}}(\mathcal{F}_s)$
 - 11: $\tilde{w}_k \leftarrow e^{w_k} / w_{sum}$
 - 12: $d \leftarrow d + \tilde{w}_k \cdot \mathcal{L}_M^e(\mathcal{F}_t, \mathcal{F}_s)$
 - 13: **end for**
 - 14: **Output** : d
-

between feature representations from the current and previous tasks, which are then incorporated into the overall loss function to maintain stability in learning.

4. Experiments

4.1. Experiment Setup

Task. We evaluate the effectiveness of our proposed method on two principal scenarios: Task Incremental Learning (Task-IL) and Class Incremental Learning (Class-IL) [50]. In the Task-IL scenario, each training task operates with an independent label space. This means that the model is trained on distinct classes for each task, allowing it to focus solely on the features relevant to the current task’s label set. During evaluation, the model receives the label space corresponding to the current task, enabling it to leverage its task-specific knowledge for accurate predictions. Conversely, in the Class-IL scenario, the tasks share a common label space. In this setup, the model must learn to classify samples from multiple tasks simultaneously, leading to a more complex learning environment. During evaluation, the model remains unaware of the specific task to which the sample belongs; instead, it must classify the sample based on the

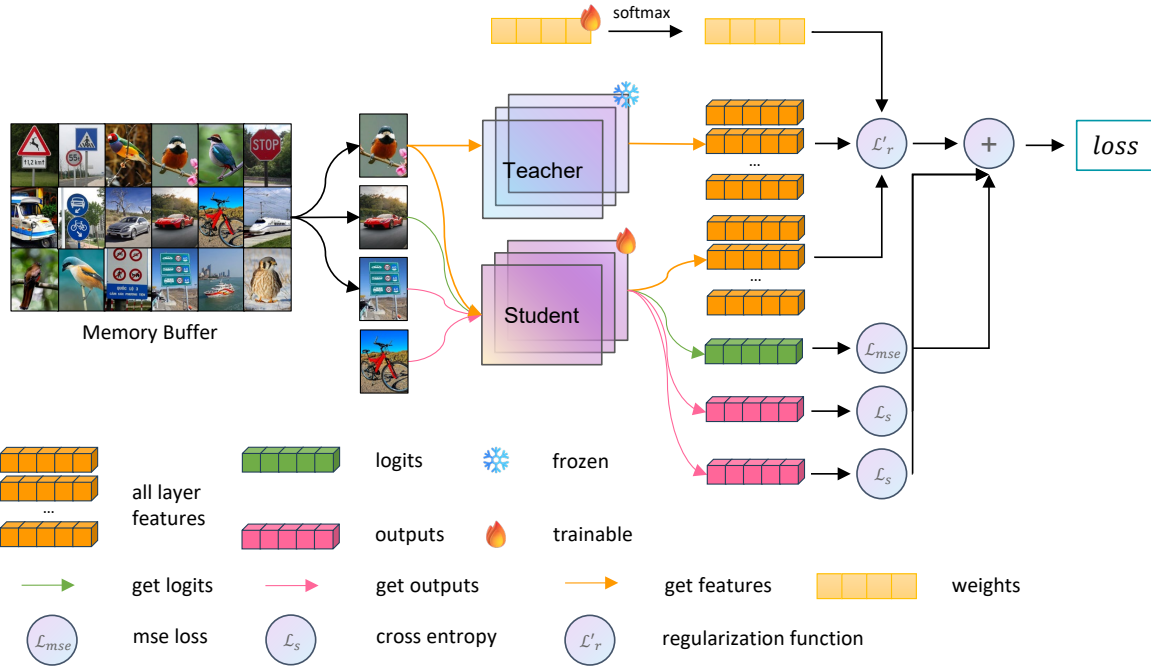


Figure 2: The learning process of the subsequent tasks, where adaptive regularization is applied to the primary loss function.

shared label space. This requires the model to generalize its learned knowledge across tasks effectively, as it cannot rely on task-specific information during inference.

We performed our experiments across multiple datasets, specifically CIFAR-10 [23] (10 classes), CIFAR-100 (100 classes), and Tiny-ImageNet (200 classes) [25]. For the CIFAR-10 dataset, we segmented it into five distinct tasks, with each task consisting of two classes. In the case of the CIFAR-100 dataset, we organized it into ten tasks, each encompassing ten classes. Additionally, for Tiny-ImageNet, we structured it into ten tasks, with each task containing twenty classes.

Implementation Details. We employ ResNet18 as our foundational architecture, comprising five layers dedicated to feature extraction. To derive the adaptive regularization optimization term, we initialized five adaptive weights randomly, sourced from a uniform distribution. Our methodology extends the code from **Refresh Learning** [54], integrating our approach within their established framework. We utilized the hyperparameters specified in their implementation and conducted a grid search to ascertain the optimal value for the γ hyperparameter, aiming to attain the most favorable outcomes.

Baseline. We conducted a comparative analysis of our proposed methodology against several contemporary baselines, which encompass regularization-based techniques such as **oEWC** [43], **Synaptic Intelligence (SI)** [65], **Learning without Forgetting (LWF)** [31], **Classifier-Projection Regularization (CPR)** [6], and **Gradient Projection Memory (GPM)** [42]. Additionally, we incorporated Bayesian approaches like **Natural Continual Learning (NCL)** [21], architecture-centric methods such as **HAT** [44], and memory-driven strategies including **ER** [10], **A-GEM** [9], **GSS** [2], **DER++** [4], and **HAL** [8]. Moreover, we also evaluated the most recent **Refresh Learning** [54] paradigm within our comparative framework.

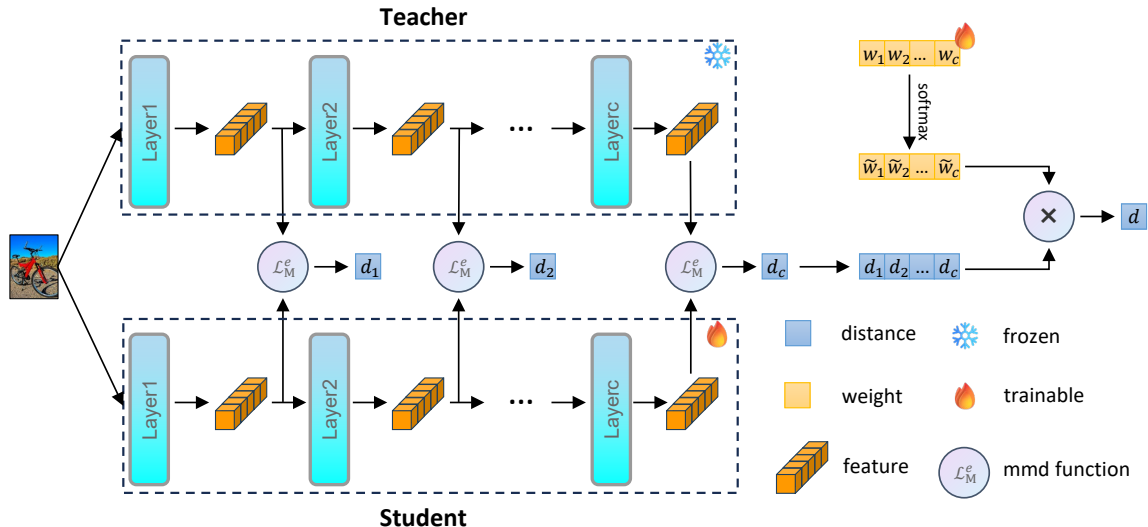


Figure 3: Illustration of the computation of the adaptive regularization term \mathcal{L}_r , showing the weighted distances between feature representations across tasks.

4.2. Comparison Results

All experiments were conducted with a memory capacity of 500. For each dataset, we executed the experiments 10 times and computed the mean accuracy along with the standard deviation. The overall accuracy for both Task-IL and Class-IL scenarios is summarized in Table.3.

Memory-based approaches, including **ER**, **A-GEM**, **GSS**, **DER++**, and **HAL**, leverage memory buffers to replay past data and mitigate catastrophic forgetting. These methods generally outperform regularization-based methods, particularly in the Task-IL scenario. For example, **ER** achieves 93.61% accuracy on CIFAR-10 under the Task-IL setting, while **DER++** and **Refresh Learning** improve this the accuracy to 93.88% and 94.44%, respectively. However, in Class-IL scenarios, these methods still struggle, with ER achieving 57.74% and DER++ improving to 72.70% on CIFAR-10. While these methods perform better than regularization-based approaches, showing that the memory-based methods are suitable for addressing network forgetting in continual learning.

Our proposed **MLFMM** method achieves the best performance across all datasets and scenarios. For CIFAR-10, **MLFMM** achieves the highest accuracy of **75.29%** under the Class-IL setting, significantly outperforming previous best-performing methods such as **DER++** (72.70%) and Refresh Learning (73.88%). Similarly, **MLFMM** achieves the highest accuracy of **94.94%** under the Task-IL setting, slightly surpassing Refresh Learning (94.44%). For the CIFAR-100 and Tiny-ImageNet, **MLFMM** consistently outperforms other methods. For example, **MLFMM** achieves **40.71%** accuracy on CIFAR-100 under the Class-IL setting, compared to 39.10% by Refresh Learning and 36.37% by **DER++**. For Tiny-ImageNet, **MLFMM** achieves **18.38%** accuracy on the Class-IL setting and **53.09%** accuracy on the Task-IL setting, demonstrating its scalability to more complex datasets.

Backward Transfer Analysis. Backward Transfer (BWT) measures the effect of

Table 3: The average accuracy of various models on 3 datasets.

Method	CIFAR-10		CIFAR-100		Tiny-ImageNet	
	Class-IL	Task-IL	Class-IL	Task-IL	Class-IL	Task-IL
fine-tuning	19.62 ± 0.05	61.02 ± 3.33	9.29 ± 0.33	33.78 ± 0.42	7.92 ± 0.26	18.31 ± 0.68
Joint train	92.20 ± 0.15	98.31 ± 0.12	71.32 ± 0.21	91.31 ± 0.17	59.99 ± 0.19	82.04 ± 0.10
SI	19.48 ± 0.17	68.05 ± 5.91	9.41 ± 0.24	31.08 ± 1.65	6.58 ± 0.31	36.32 ± 0.13
CPR(EWC)	19.61 ± 3.67	65.23 ± 3.87	8.42 ± 0.37	21.43 ± 2.57	7.67 ± 0.23	15.58 ± 0.91
LWF	19.61 ± 0.05	63.29 ± 2.35	9.70 ± 0.23	28.07 ± 1.96	8.46 ± 0.22	15.85 ± 0.58
GPM	-	90.68 ± 3.29	-	72.48 ± 0.40	-	-
oEWC	19.49 ± 0.12	64.31 ± 4.31	8.24 ± 0.21	21.2 ± 2.08	7.42 ± 0.31	15.19 ± 0.82
NCL	19.53 ± 0.32	64.49 ± 4.06	8.12 ± 0.28	20.92 ± 2.32	7.56 ± 0.36	16.29 ± 0.87
HAT	-	92.56 ± 0.78	-	72.06 ± 0.50	-	-
UCB	-	79.28 ± 1.87	-	57.15 ± 1.67	-	-
HAL	41.79 ± 4.46	84.54 ± 2.36	9.05 ± 2.76	42.94 ± 1.80	-	-
A-GEM	22.67 ± 0.57	89.48 ± 1.45	9.30 ± 0.32	48.06 ± 0.57	8.06 ± 0.04	25.33 ± 0.49
GSS	49.73 ± 4.78	91.02 ± 1.57	13.60 ± 2.98	57.50 ± 1.93	-	-
ER	57.74 ± 0.27	93.61 ± 0.27	20.98 ± 0.35	73.37 ± 0.43	9.99 ± 0.29	48.64 ± 0.46
DER++	72.70 ± 1.36	93.88 ± 0.50	36.37 ± 0.85	75.64 ± 0.60	19.38 ± 1.41	51.91 ± 0.68
refresh	73.88 ± 1.16	94.44 ± 0.39	39.10 ± 0.65	76.80 ± 0.31	16.16 ± 0.72	53.36 ± 1.25
MLFMM	75.29 ± 0.75	94.94 ± 0.41	40.71 ± 0.61	76.86 ± 0.82	18.38 ± 0.31	53.69 ± 0.93

learning new tasks. Negative values indicate a decline in performance on earlier tasks after training on new tasks, highlighting the challenge of catastrophic forgetting in continual learning. Table 4 presents the BWT scores of various methods across three datasets: CIFAR-10, CIFAR-100 and Tiny-ImageNet, in both Class-IL and Task-IL scenarios. From the results of Table 4, we can observe that the fine-tuning achieves the worst BWT across all datasets, with highly negative values in both Class-IL and Task-IL scenarios. For instance, fine-tuning achieves a BWT of -96.39% and -46.24% for Class-IL and Task-IL on CIFAR-10, respectively. This confirms that without strategies to mitigate forgetting, the network overwrites its knowledge of previous tasks while learning new ones.

Regularization-based approaches, including **A-GEM** and **GSS** slightly improve backward transfer but still struggle with catastrophic forgetting. For example, AGEM achieves -94.01% BWT in Class-IL for CIFAR-10, which is only marginally better than finetuning.

Memory-based methods such as **HAL**, **ER**, and **DER++** perform better in reducing BWT. Among these, **DER++** and **Refresh** achieve -22.38 and -22.03 BWT values on CIFAR-10 under the Class-IL setting, demonstrating notable improvements compared to other baselines. In addition, the proposed **MLFMM** achieves the best backward transfer across all datasets and scenarios. For example: On CIFAR-10, OW-MMD achieves a backward transfer of -20.61 in Class-IL and -3.0 in Task-IL, outperforming both **DER++** and **Refresh**. For CIFAR-100, OW-MMD achieves -42.99 and -13.8 under the Class-IL and Task-IL setting, respectively, which are significantly better than **DER++** and other baselines. For the more complex dataset such as Tiny-ImageNet, OW-MMD also demonstrates better backward transfer with -59.31 and -27.73 under the Class-IL and Task-IL settings, outperforming most baselines such as **DER++** and **Refresh**.

Table 4: Backward Transfer of various methods on 3 datasets with buffer size 500.

Method	CIFAR-10		CIFAR-100		Tiny-ImageNet	
	Class-IL	Task-IL	Class-IL	Task-IL	Class-IL	Task-IL
finetuning	-96.39±0.12	-46.24±2.12	-89.68±0.96	-62.46±0.78	-78.94±0.81	-67.34±0.79
HAL	-62.21±4.34	-5.41±1.10	-49.29±2.82	-13.60±1.04	-	-
AGEM	-94.01±1.16	-14.26±1.18	-88.5±1.56	-45.43±2.32	-78.03±0.78	-59.28±1.08
GSS	-62.88±2.67	-7.73±3.99	-82.17±4.16	-33.98±1.54	-	-
ER	-45.35±0.07	-3.54±0.35	-74.84±1.38	-16.81±0.97	-75.24±0.76	-31.98±1.35
DER++	-22.38±4.41	-4.66±1.15	-53.89±1.85	-14.72±0.96	-64.6±0.56	-27.21±1.23
refresh	-22.03±3.89	-4.37±1.25	-53.51±0.70	-14.23±0.75	-63.90±0.61	-25.05±1.05
MLFMM	-20.61±0.45	-3.0 ± 0.48	-42.99±1.23	-13.8±0.84	-59.31±0.64	-27.73±1.0

4.3. Analysis Results

Forgetting Curve. Forgetting rates highlights the extent of knowledge loss over time. In this analysis, we investigate the forgetting curves for several methods. The forgetting curves for Class-IL and Task-IL settings are shown in 4, which demonstrate significant differences in performance across various methods.

For the class-incremental learning scenario, methods such as **DER**, **DER++**, and **ER** demonstrate relatively slow forgetting, with the forgetting rate steadily increasing as more tasks are learned, but remaining at manageable levels. Notably, **DER** and **DER++** show smaller increments in forgetting compared to **ER**, indicating the effectiveness of their more advanced replay strategies combined with knowledge distillation and regularization. In contrast, **oEWC** and **LWF** exhibit a significant rise in forgetting, particularly in later tasks, highlighting the challenges of using regularization methods alone without the aid of rehearsal or distillation. The forgetting rates for these methods indicate substantial memory loss, as their performance on earlier tasks degrades significantly when new tasks are introduced.

In the task-incremental learning setup, the methods show a similar trend, although the forgetting rates are generally lower compared to the class-incremental scenario due to the more explicit task boundaries. **DER** and **DER++** continue to perform well, showing relatively stable forgetting curves with only slight increases in forgetting over time. **ER** also performs reasonably well, though it demonstrates a slightly higher increase in forgetting rates as the number of tasks increases. The **oEWC** and **LWF** methods again suffer from greater forgetting, with their forgetting rates increasing more rapidly as new tasks are added. However, our **MLFMM** method shows the best performance across both scenarios, with its forgetting curve remaining relatively flat throughout the learning process. This indicates that **MLFMM**, supported by its adaptive regularization optimization, is highly effective in mitigating catastrophic forgetting, achieving stability even as new tasks are added.

In summary, the analysis of the forgetting curves reveals that while methods such as **DER**, **DER++**, and **ER** provide effective solutions to mitigate forgetting, **oEWC** and **LWF** struggle to maintain task performance over time. The proposed **MLFMM** framework, however, stands out for its ability to minimize forgetting effectively across both class-incremental and task-incremental learning scenarios. This highlights the potential of combining multi-level feature matching with adaptive regularization to

tackle the challenge of catastrophic forgetting in continual learning

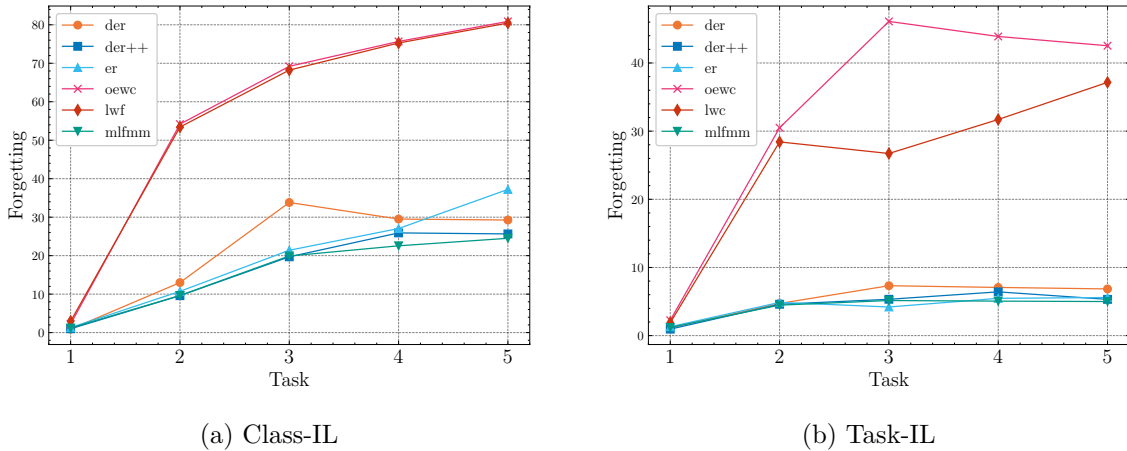


Figure 4: The forgetting curves for Class-Incremental Learning (a) and Task-Incremental Learning (b) on CIFAR10.

Optimal Weight Analysis. In the proposed adaptive regularization optimization term, as described in Section 3.4, we introduce adaptive weights for each network layer. These weights are dynamically adjusted to optimize knowledge transfer between the teacher and student networks. During each task learning, the model can determine the optimal weights specific to the current task. These weights are updated and refined as the network progresses through subsequent tasks, ensuring continuous improvement in the learning process.

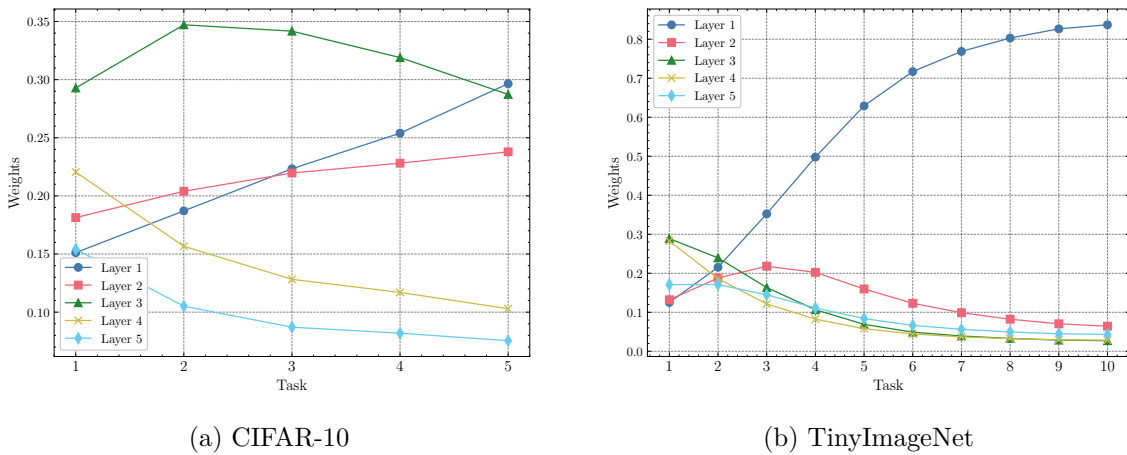


Figure 5: Evolution of Weights Across Tasks for Different Layers. The figure illustrates how the weights assigned to different network layers evolve as tasks progress, showing the increasing importance of shallow layers and the decreasing trend in deep layers.

The evolution of these weights across tasks is illustrated in Fig 5. From these results, we can find several trends, summarized in the following :

1. **Shallow Layers:** The weights assigned to the shallower layers tend to increase as the tasks progress. This increase suggests that the network relies more heavily on basic, lower-level features as new tasks are introduced. These shallow layers

capture fundamental representations, such as edges and textures, which are generally useful across different tasks, providing semantically rich information that supports continual learning.

2. **Deep Layers:** The weights for deeper layers show a decreasing trend across both datasets. This result indicates that as more tasks are added, the network becomes less dependent on features extracted by these deeper layers. This reflects the need to retain generalized knowledge that is applicable across a range of tasks rather than retaining highly specialized features, which may be less transferable.
3. **Mid-Level Layers:** The mid-level layers demonstrate an initial increase in weight, followed by a decline as training progresses. For instance, Layer 3 in CIFAR-10 and Layer 2 in Tiny-ImageNet both initially gain importance as the network learns to handle the variety of tasks introduced early on. This increase occurs because these layers capture moderately complex features that are valuable during the initial stages of learning. However, as more tasks are introduced, these mid-level features become less significant compared to the foundational representations provided by the shallow layers. The eventual decline in mid-level layer importance reflects the network’s shift towards retaining the most stable and general features over task-specific knowledge.

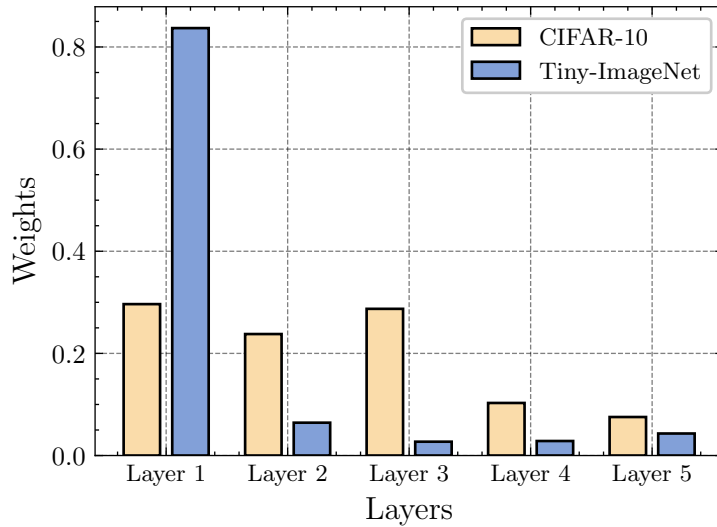


Figure 6: Final Weight Distribution Across Layers After Completing All Tasks. The bar chart shows the final distribution of weights for different layers of the network across datasets, highlighting that the optimal weight distribution varies between different datasets. This illustrates the different levels of importance assigned to each layer depending on the characteristics of the dataset.

The bar graph in Figure 6 illustrates the final distribution of adaptive weights between the different layers of the network after completing all tasks. It is evident that the optimal weight distribution varies significantly between datasets such as CIFAR-10 and Tiny-ImageNet. For CIFAR-10, the network tends to assign higher weights to certain shallow layers, indicating their importance in generalizing across tasks. On the other hand, for Tiny-ImageNet, the weight distribution is more concentrated towards specific layers, reflecting the dataset’s complexity and the unique feature extraction requirements. These differences highlight how the network adapts its internal representations depending on the characteristics of the dataset, dynamically adjusting the importance

Table 5: Comparison of distance functions and the effect of optimal weights on CIFAR-10 with buffer size 500

dist_fun	AROT	Class-IL	Task-IL
cos	F	74.62±0.79	94.53±0.18
cos	T	74.89±0.86	94.67±0.27
L2	F	75.12±0.74	94.88±0.33
L2	T	75.23±0.94	94.56±0.15
mmd	F	74.69±1.07	94.51±0.24
mmd	T	75.29±0.75	94.94±0.41

Table 6: The average accuracy of various buffer size on CIFAR10.

Buffer Size Method	200		5120	
	Class-IL	Task-IL	Class-IL	Task-IL
GEM	25.54±0.76	90.44±0.94	25.26±3.46	95.55±0.02
iCaRL	49.02±3.20	88.99±2.13	55.07±1.55	92.23±0.84
FDR	30.91±2.74	91.01±0.68	19.70±0.07	94.32±0.97
HAL	32.36±2.70	82.51±3.20	59.12±4.41	88.51±3.32
A-GEM	20.04±0.34	83.88±1.49	21.99±2.29	90.10±2.09
GSS	39.07±5.59	88.80±2.89	67.27±4.27	94.19±1.15
ER	44.79±1.86	91.19±0.94	82.47±0.52	96.98±0.17
DER++	64.88±1.17	91.92±0.60	85.24±0.49	96.12±0.21
refresh	65.39±1.01	92.80±0.42	85.98±0.43	96.43±0.11
MLFMM	67.74±1.06	92.97±0.37	86.33±0.37	96.61±0.13

of each layer to optimize knowledge retention and transfer in a continual learning setting.

Distance Function Analysis. Table 5 compares the performance of different distance functions and the effect of using optimal weights in our experiments on CIFAR-10 with a buffer size of 500. The first column represents the distance function used, while the second column indicates whether adaptive regularization optimization term (AROT) were applied, with "F" denoting no use of adaptive weights and "T" indicating their use.

From the results, it is evident that using the Maximum Mean Discrepancy (MMD) distance function yields the best performance in both the Class-IL and Task-IL scenarios. Specifically, the configuration with MMD and adaptive weights achieves the highest accuracy. Additionally, we observe that for the same distance function, the use of adaptive weights consistently outperforms the fixed weight configurations. This demonstrates the effectiveness of both MMD as a distance function and the benefits of applying adaptive weights to improve performance during continual learning.

Buffer Size. Table 6 shows the performance of our proposed MLFMM method with different buffer sizes and compares it with several other continual learning methods. We evaluate the accuracy of each method on the CIFAR10 dataset under both Class-IL and Task-IL settings, using buffer sizes of 200 and 5120.

For the smaller buffer size (200), MLFMM achieves the highest accuracy in both Class-IL and Task-IL settings. Specifically, MLFMM outperforms other methods with a Class-

IL accuracy of 67.74% and a Task-IL accuracy of 92.97%, which is better than any other method in this scenario. Other methods, such as GEM and A-GEM, perform relatively poorly with this smaller buffer, showing significantly lower accuracies, especially in the Class-IL setting. MLFMM’s superior performance indicates its ability to leverage smaller memory buffers effectively, which is crucial for real-world applications with limited memory.

When we increase the buffer size to 5120, MLFMM continues to perform well, although its performance advantage over other methods becomes less pronounced. In this larger buffer setting, ER and DER++ achieve slightly higher Task-IL accuracies (96.98% and 96.12%, respectively) than MLFMM’s 96.61%, while MLFMM still outperforms other methods in Class-IL. This demonstrates that MLFMM remains competitive with larger buffer sizes and continues to offer strong performance, especially in the Class-IL scenario.

In conclusion, MLFMM excels in both small and large buffer settings, particularly in Class-IL scenarios. It offers a balanced trade-off between performance and memory usage, outperforming many popular continual learning methods across different buffer sizes. These results highlight the potential of MLFMM for continual learning tasks with constrained memory budgets.

Training Time Comparison. We analyze the training times of our proposed MLFMM method in comparison with other baseline methods. The training time data for each method is shown in Figure 7. As observed, the training time for MLFMM is notably higher than most of the other methods. Specifically, MLFMM takes approximately 143 minutes, which is significantly longer than methods such as oEWC (28 minutes), LWF (32 minutes), and ER (40 minutes). However, the method still performs competitively when considering the effectiveness of the results, demonstrating a balance between computational cost and model performance. The GSS method, while highly effective, has the longest training time at 300 minutes, which suggests a trade-off between performance and efficiency. Despite the higher time cost, the MLFMM method achieves promising results in terms of accuracy and memory retention.

4.4. Ablation Study

In this section, we perform an ablation study to evaluate the individual contributions of the three terms— α -term, β -term, and γ -term—in our proposed method. The aim is to investigate how each component influences the overall performance and identify the most critical factors for improving continual learning.

We systematically test different combinations of these terms in the loss function. These experiments are conducted using a memory buffer size of 500 on the CIFAR-10 dataset. The results are summarized in the Table 7 below:

Base Model. This variant only includes the standard loss function without any of the additional terms (α -term, β -term, or γ -term). This helps establish a baseline performance for comparison. The base model performs very poorly because it does not incorporate any continual learning strategies, resulting in catastrophic forgetting.

α -term, β -term, and γ -term. In this configuration, we evaluate the individual contributions of the α -term (logits matching), β -term (label replay), and γ -term (teacher-

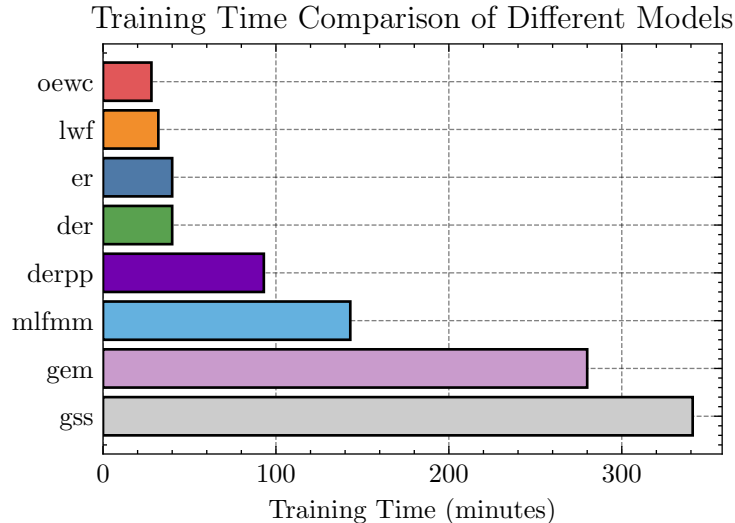


Figure 7: Training time comparison of different models (in minutes). The bar plot shows the runtime for each model during training, indicating significant variation in the computational cost across different methods.

Table 7: Ablation study results on CIFAR-10 with buffer size 500

Term	Class-IL	Task-IL
base	19.62±0.33	61.02±0.24
α	70.26±0.33	93.31±0.18
β	66.04±2.54	94.18±0.29
γ	19.62±0.04	84.56±4.84
$\alpha + \beta$	73.88±1.16	94.44±0.41
$\alpha + \gamma$	73.53±1.21	93.81±0.31
$\beta + \gamma$	69.53±1.33	94.99±0.09
$\alpha + \beta + \gamma$	75.29±0.75	94.94±0.41

student transfer). The results show that the inclusion of only the α -term or the β -term, both of which involve using the memory buffer, already yields good performance. However, when only the γ -term is used, the performance is poor. This is because the teacher-student method relies on a strong teacher network, and in the absence of the memory buffer, the teacher also suffers from catastrophic forgetting.

Combination of two terms. When two terms are combined, the results are better than when any single term is used individually. Specifically, combining the α -term and β -term (logits matching and label replay) leads to improved performance, as both terms utilize the memory buffer to preserve past knowledge. Similarly, combining the α -term and γ -term (logits matching and teacher-student transfer) also results in better performance compared to using either term alone, as it ensures both alignment with previous experiences and the knowledge transfer from the teacher network. This demonstrates the complementary nature of these terms in mitigating catastrophic forgetting.

Full Model. This final configuration includes all three terms (α , β , and γ) as in our proposed method. It represents the complete approach and serves as the optimal model for comparison.

5. Conclusion and Future Works

In this paper, we introduce an innovative framework for alleviating catastrophic forgetting in continual learning, called Optimally-Weighted Maximum Mean Discrepancy (OWMMD). Specifically, the proposed framework introduces a Multi-Level Feature Matching Mechanism (MLFMM) to penalize representation changes in order to relieve network forgetting. This technique utilizes various layers of neural networks to ensure coherence between the feature representations of prior and current tasks. By integrating a regularization term that reduces the disparity between feature representations across different tasks, our methodology illustrates the capability to avert catastrophic forgetting while facilitating the model’s adaptation to a dynamic data stream.

The empirical findings indicate that our methodology surpasses current techniques regarding both precision and consistency across various tasks. By modulating the feature space and accommodating new tasks while preserving previously acquired knowledge, our approach enhances the expanding literature on continual learning. Furthermore, the incorporation of probabilistic distance metrics in feature alignment offers a promising avenue for advancing task generalization and transfer learning.

While promising, there are several areas where this work can be expanded in future research. First, the efficiency of memory buffer management and sample selection can be further optimized by exploring more advanced sampling strategies or leveraging external memory architectures. Second, our method’s performance on larger-scale datasets and in real-world applications, such as robotics or autonomous driving, remains to be fully explored. Finally, extending our feature-matching approach to other types of neural architectures, such as transformer-based models or generative networks, could provide broader applicability and improve performance across a wider range of tasks.

In summary, this work lays the foundation for more robust continual learning systems that can efficiently retain and transfer knowledge across multiple tasks. Future work will focus on refining the proposed methods, exploring additional regularization techniques, and evaluating the approach in more complex settings to advance the state-of-the-art in continual learning.

References

- [1] R. Aljundi, P. Chakravarty, and T. Tuytelaars. Expert gate: Lifelong learning with a network of experts. In *Proc. of the IEEE Conf. on Computer Vision and Pattern Recognition (CVPR)*, pages 3366–3375, 2017.
- [2] Rahaf Aljundi, Min Lin, Baptiste Goujaud, and Yoshua Bengio. Gradient based sample selection for online continual learning. In *Advances in Neural Information Processing Systems 32, Volume 15 of 20: 32nd Conference on Neural Information Processing Systems (NeurIPS 2019). Vancouver(CA).8-14 December 2019*, 2020.
- [3] Jihwan Bang, Heesu Kim, YoungJoon Yoo, Jung-Woo Ha, and Jonghyun Choi. Rainbow memory: Continual learning with a memory of diverse samples. In *Proc. of IEEE/CVF Conf. on Computer Vision and Pattern Recognition (CVPR)*, pages 8218–8227, 2021.

- [4] Matteo Buzzega, Pietro and Boschini, Angelo Porrello, Davide Abati, and Simone Calderara. Dark experience for general continual learning: a strong, simple baseline. In *Advances in Neural Information Processing Systems (NIPS)*, pages 15920–15930, 2020.
- [5] Hyuntak Cha, Jaeho Lee, and Jinwoo Shin. Co2l: Contrastive continual learning. In *Proceedings of the IEEE/CVF International conference on computer vision*, pages 9516–9525, 2021.
- [6] Sungmin Cha, Hsiang Hsu, Taebaek Hwang, Flavio P Calmon, and Taesup Moon. Cpr: classifier-projection regularization for continual learning. *arXiv preprint arXiv:2006.07326*, 2020.
- [7] Arslan Chaudhry, Puneet K. Dokania, Thalaiyasingam Ajanthan, and Philip H. S. Torr. *Riemannian Walk for Incremental Learning: Understanding Forgetting and Intransigence*, page 556–572. Springer International Publishing, 2018.
- [8] Arslan Chaudhry, Albert Gordo, Puneet Dokania, Philip Torr, and David Lopez-Paz. Using hindsight to anchor past knowledge in continual learning. In *Proceedings of the AAAI Conference on Artificial Intelligence*, volume 35, pages 6993–7001, 2021.
- [9] Arslan Chaudhry, Marc’Aurelio Ranzato, Marcus Rohrbach, and Mohamed Elhoseiny. Efficient lifelong learning with a-gem, 2019.
- [10] Arslan Chaudhry, Marcus Rohrbach, Mohamed Elhoseiny, Thalaiyasingam Ajanthan, Puneet K. Dokania, Philip H. S. Torr, and Marc’Aurelio Ranzato. On tiny episodic memories in continual learning, 2019.
- [11] Z. Chen, N. Ma, and B. Liu. Lifelong learning for sentiment classification. In *Proc. of the Annual Meeting of the Assoc. for Comp. Linguistics and Int. Joint Conf. on Natural Language Processing*, pages 750–756, 2015.
- [12] Andrea Cossu, Antonio Carta, Vincenzo Lomonaco, and Davide Bacciu. Continual learning for recurrent neural networks: an empirical evaluation. *Neural Networks*, 143:607–627, 2021.
- [13] Arthur Douillard, Alexandre Ramé, Guillaume Couairon, and Matthieu Cord. Dyttox: Transformers for continual learning with dynamic token expansion. In *Proceedings of the IEEE/CVF Conference on Computer Vision and Pattern Recognition (CVPR)*, pages 9285–9295, June 2022.
- [14] Gintare Karolina Dziugaite, Daniel M Roy, and Zoubin Ghahramani. Training generative neural networks via maximum mean discrepancy optimization. *arXiv preprint arXiv:1505.03906*, 2015.
- [15] Robert M French. Catastrophic forgetting in connectionist networks. *Trends in cognitive sciences*, 3(4):128–135, 1999.

- [16] Qiankun Gao, Chen Zhao, Yifan Sun, Teng Xi, Gang Zhang, Bernard Ghanem, and Jian Zhang. A unified continual learning framework with general parameter-efficient tuning. In *Proceedings of the IEEE/CVF International Conference on Computer Vision*, pages 11483–11493, 2023.
- [17] Jianping Gou, Baosheng Yu, Stephen J Maybank, and Dacheng Tao. Knowledge distillation: A survey. *International Journal of Computer Vision*, 129(6):1789–1819, 2021.
- [18] Yanan Gu, Xu Yang, Kun Wei, and Cheng Deng. Not just selection, but exploration: Online class-incremental continual learning via dual view consistency. In *Proc. of the IEEE/CVF Conference on Computer Vision and Pattern Recognition (CVPR)*, pages 7442–7451, June 2022.
- [19] Ya-nan Han and Jian-wei Liu. Online continual learning via the meta-learning update with multi-scale knowledge distillation and data augmentation. *Engineering Applications of Artificial Intelligence*, 113:104966, 2022.
- [20] Geoffrey Hinton. Distilling the knowledge in a neural network. *arXiv preprint arXiv:1503.02531*, 2015.
- [21] Ta-Chu Kao, Kristopher Jensen, Gido van de Ven, Alberto Bernacchia, and Guillaume Hennequin. Natural continual learning: success is a journey, not (just) a destination. *Advances in neural information processing systems*, 34:28067–28079, 2021.
- [22] J. Kirkpatrick, R. Pascanu, N. Rabinowitz, J. Veness, G. Desjardins, A. A. Rusu, K. Milan, J. Quan, T. Ramalho, A. Grabska-Barwinska, D. Hassabis, C. Clopath, D. Kumaran, and R. Hadsell. Overcoming catastrophic forgetting in neural networks. *Proc. of the National Academy of Sciences (PNAS)*, 114(13):3521–3526, 2017.
- [23] Alex Krizhevsky and Geoffrey Hinton. Learning multiple layers of features from tiny images. Technical report, Univ. of Toronto, 2009.
- [24] Richard Kurle, Botond Cseke, Alexej Klushyn, Patrick van der Smagt, and Stephan Günnemann. Continual learning with bayesian neural networks for non-stationary data. In *Proc. Int. Conf. on Learning Representations (ICLR)*, 2020.
- [25] Yann Le and Xuan Yang. Tiny imagenet visual recognition challenge. *CS 231N*, 7:3, 2015.
- [26] Y. LeCun, L. Bottou, Y. Bengio, and P. Haffner. Gradient-based learning applied to document recognition. *Proc. of the IEEE*, 86(11):2278–2324, 1998.
- [27] Sebastian Lee, Sebastian Goldt, and Andrew Saxe. Continual learning in the teacher-student setup: Impact of task similarity. In *International Conference on Machine Learning*, pages 6109–6119. PMLR, 2021.
- [28] Hongbo Li, Sen Lin, Lingjie Duan, Yingbin Liang, and Ness B. Shroff. Theory on mixture-of-experts in continual learning, 2024.

- [29] Jin Li, Zhong Ji, Gang Wang, Qiang Wang, and Feng Gao. Learning from students: Online contrastive distillation network for general continual learning. In *IJCAI*, pages 3215–3221, 2022.
- [30] Xiaorong Li, Shipeng Wang, Jian Sun, and Zongben Xu. Variational data-free knowledge distillation for continual learning. *IEEE Transactions on Pattern Analysis and Machine Intelligence*, 45(10):12618–12634, 2023.
- [31] Z. Li and D. Hoiem. Learning without forgetting. *IEEE Trans. on Pattern Analysis and Machine Intelligence*, 40(12):2935–2947, 2017.
- [32] David Lopez-Paz and Marc’Aurelio Ranzato. Gradient episodic memory for continual learning, 2022.
- [33] Arun Mallya and Svetlana Lazebnik. Packnet: Adding multiple tasks to a single network by iterative pruning, 2018.
- [34] Nicolas Michel, Maorong Wang, Ling Xiao, and Toshihiko Yamasaki. Rethinking momentum knowledge distillation in online continual learning, 2024.
- [35] G. I. Parisi, R. Kemker, J. L. Part, C. Kanan, and S. Wermter. Continual lifelong learning with neural networks: A review. *Neural Networks*, 113:54–71, 2019.
- [36] German I. Parisi, Ronald Kemker, Jose L. Part, Christopher Kanan, and Stefan Wermter. Continual lifelong learning with neural networks: A review. *Neural Networks*, 113:54–71, 2019.
- [37] Dabal Pedamonti. Comparison of non-linear activation functions for deep neural networks on mnist classification task. *arXiv preprint arXiv:1804.02763*, 2018.
- [38] Quang Pham, Chenghao Liu, and Steven C. H. Hoi. Continual learning, fast and slow, 2023.
- [39] Sylvestre-Alvise Rebuffi, Alexander Kolesnikov, and Christoph H. Lampert. icarl: Incremental classifier and representation learning. *CoRR*, abs/1611.07725, 2016.
- [40] Adriana Romero, Nicolas Ballas, Samira Ebrahimi Kahou, Antoine Chassang, Carlo Gatta, and Yoshua Bengio. Fitnets: Hints for thin deep nets. *arXiv preprint arXiv:1412.6550*, 2014.
- [41] Andrei A Rusu, Neil C Rabinowitz, Guillaume Desjardins, Hubert Soyer, James Kirkpatrick, Koray Kavukcuoglu, Razvan Pascanu, and Raia Hadsell. Progressive neural networks. *arXiv preprint arXiv:1606.04671*, 2016.
- [42] Gobinda Saha, Isha Garg, and Kaushik Roy. Gradient projection memory for continual learning. *arXiv preprint arXiv:2103.09762*, 2021.
- [43] Jonathan Schwarz, Jelena Luketina, Wojciech M. Czarnecki, Agnieszka Grabska-Barwinska, Yee Whye Teh, Razvan Pascanu, and Raia Hadsell. Progress & compress: A scalable framework for continual learning, 2018.

- [44] Joan Serra, Dídac Surís, Marius Miron, and Alexandros Karatzoglou. Overcoming catastrophic forgetting with hard attention to the task, 2018.
- [45] Neha Sharma, Vibhor Jain, and Anju Mishra. An analysis of convolutional neural networks for image classification. *Procedia computer science*, 132:377–384, 2018.
- [46] Hanul Shin, Jung Kwon Lee, Jaehong Kim, and Jiwon Kim. Continual learning with deep generative replay. *Advances in neural information processing systems*, 30, 2017.
- [47] Alexander J Smola, A Gretton, and K Borgwardt. Maximum mean discrepancy. In *13th international conference, ICONIP*, pages 3–6, 2006.
- [48] Filip Szatkowski, Mateusz Pyla, Marcin Przewięźlikowski, Sebastian Cygert, Bartłomiej Twardowski, and Tomasz Trzcíński. Adapt your teacher: Improving knowledge distillation for exemplar-free continual learning. In *Proceedings of the IEEE/CVF Winter Conference on Applications of Computer Vision*, pages 1977–1987, 2024.
- [49] Ilya O Tolstikhin, Bharath K Sriperumbudur, and Bernhard Schölkopf. Minimax estimation of maximum mean discrepancy with radial kernels. *Advances in Neural Information Processing Systems*, 29:1930–1938, 2016.
- [50] Guido M Van, de Ven and Andreas S Tolas. Three scenarios for continual learning. *NeurIPS Continual Learning Workshop*, 2019.
- [51] Jeffrey S Vitter. Random sampling with a reservoir. *ACM Transactions on Mathematical Software (TOMS)*, 11(1):37–57, 1985.
- [52] Liyuan Wang, Xingxing Zhang, Hang Su, and Jun Zhu. A comprehensive survey of continual learning: Theory, method and application. *IEEE Transactions on Pattern Analysis and Machine Intelligence*, 46(8):5362–5383, 2024.
- [53] X. Wang, R. Zhang, Y. Sun, and J. Qi. KDGAN: knowledge distillation with generative adversarial networks. In *Proc. Advances in Neural Inf. Proc. Systems (NIPS)*, pages 775–786, 2018.
- [54] Zhenyi Wang, Yan Li, Li Shen, and Heng Huang. A unified and general framework for continual learning, 2024.
- [55] Zifeng Wang, Zizhao Zhang, Chen-Yu Lee, Han Zhang, Ruoxi Sun, Xiaoqi Ren, Guolong Su, Vincent Perot, Jennifer Dy, and Tomas Pfister. Learning to prompt for continual learning. In *Proceedings of the IEEE/CVF Conference on Computer Vision and Pattern Recognition (CVPR)*, pages 139–149, June 2022.
- [56] Zifeng Wang, Zizhao Zhang, Chen-Yu Lee, Han Zhang, Ruoxi Sun, Xiaoqi Ren, Guolong Su, Vincent Perot, Jennifer Dy, and Tomas Pfister. Learning to prompt for continual learning. In *Proceedings of the IEEE/CVF conference on computer vision and pattern recognition*, pages 139–149, 2022.

- [57] Buddhi Wickramasinghe, Gobinda Saha, and Kaushik Roy. Continual learning: A review of techniques, challenges and future directions. *IEEE Transactions on Artificial Intelligence*, 2023.
- [58] Buddhi Wickramasinghe, Gobinda Saha, and Kaushik Roy. Continual learning: A review of techniques, challenges, and future directions. *IEEE Transactions on Artificial Intelligence*, 5(6):2526–2546, 2024.
- [59] Qingsen Yan, Dong Gong, Yuhang Liu, Anton van den Hengel, and Javen Qinfeng Shi. Learning bayesian sparse networks with full experience replay for continual learning. In *Proc. of the IEEE/CVF Conference on Computer Vision and Pattern Recognition (CVPR)*, pages 109–118, 2022.
- [60] Fei Ye and Adrian G. Bors. Lifelong learning of interpretable image representations. In *Proc. Int. Conf. on Image Processing Theory, Tools and Applications (IPTA)*, pages 1–6, 2020.
- [61] Fei Ye and Adrian G. Bors. Continual compression model for online continual learning. *Applied Soft Computing*, 167:112427, 2024.
- [62] Fei Ye and Adrian. G. Bors. Self-supervised adversarial variational learning. *Pattern Recognition*, 148:110156, 2024.
- [63] Fei Ye and Adrian G Bors. Task-free dynamic sparse vision transformer for continual learning. In *Proceedings of the AAAI Conference on Artificial Intelligence*, volume 38, pages 16442–16450, 2024.
- [64] J. Yoon, E. Yang, J. Lee, and S. J. Hwang. Lifelong learning with dynamically expandable networks. In *Proc. Int. Conf. on Learning Representations (ICLR)*, *arXiv preprint arXiv:1708.01547*, 2017.
- [65] F. Zenke, B. Poole, and S. Ganguli. Continual learning through synaptic intelligence. In *Proc. of Int. Conf. on Machine Learning, vol. PLMR 70*, pages 3987–3995, 2017.